

ONLINE-CAPABLE CLEANING OF HIGHLY ARTEFACTUAL EEG DATA RECORDED DURING REAL DRIVING

L.R. Krol¹, T.O. Zander¹, M. Jaswa², O. Flascher², A. Snelting³, A-M. Brouwer³

¹ Zander Laboratories B.V., Amsterdam, Netherlands

² DCS Corporation, Alexandria, VA, United States

³ Netherlands Organization for Applied Scientific Research (TNO), Soesterberg, Netherlands

E-mail: lrkrol@gmail.com

ABSTRACT: With an increased interest to develop brain-computer interface (BCI) applications that can be used in real-world contexts, comes an increased need to deal with the myriad sources of artefacts that interfere with the signal of interest. We present real-world data recorded in a moving car, contaminated with muscle artifacts, mechanical artifacts, and noise produced by the car's electrical systems. We use artifact subspace reconstruction and independent component analysis to rigorously clean and filter the data. We demonstrate that using state-of-the-art methods, it is possible to identify cortical processes even in heavily contaminated data.

INTRODUCTION

A number of current developments in brain-computer interface (BCI) research point towards an increased interest in real-world implementations. We see the development of easy-to-apply, commercial, dry electrode systems [1-3] as well as a number of wireless, mobile solutions for BCI [4-5]. These developments are no longer aimed at neurophysiological research per se, nor limited to support motor-impaired users. Also the ongoing proliferation of passive BCI [6-7], where BCI is used by individuals without disabilities to support ongoing human-computer interaction, indicates an increased interest in applying BCI to real-world scenarios, outside of the experimental laboratory.

At the same time, developments in other areas are showing a clear need for information reflecting a user's cognitive or affective state. As systems become increasingly automated, researchers attempt to make the automated adaptation match the needs and preferences of the individual user. As these may vary between contexts and over time, it is important that this information can be assessed in real time within the given context [8]. Such information can be provided using passive BCI methodology. This can be fed into *neuroadaptive* [9] systems as implicit input [10], enabling them to support their users in a timely and individualized fashion.

One drawback of real-world scenarios is that they cannot be experimentally controlled. For EEG-based BCI in particular, the presence of electromagnetically active sources may interfere with or obscure the signal of interest. On top of that, users of real-world applications tend not to sit motionless for the duration of the activity.

Thus, the myoelectric signals produced by the contracting shoulder, neck, and facial muscles contaminate the EEG recording. These movements as well as displacements of the equipment itself may also introduce mechanical artifacts in the EEG recording.

We focus here on the real-world use scenario of an autonomously driving car. The use of in-car EEG and BCI have recently been investigated by e.g. [11-14], establishing that state detection is possible, although the signal-to-noise ratio is low due to environmental noise and movement artefacts. Here, we focus on rigorous cleaning methods in order to implement neuroadaptivity in the context of autonomous driving.

There is an increasing prevalence of automated driving systems taking over drivers' tasks. While there are clear benefits to this in terms of comfort and safety, the human driver is more and more disconnected from the activity and left out of the loop. The behavior of current automated driving systems could benefit from additional information concerning the human driver's perspective. That way, the human brain can serve as an additional sensor for the car, allowing the car to adapt to the needs and wishes of human driver. The driver can be implicitly kept in the human-machine interaction loop, and the car can benefit from the continuous, context-sensitive implicit input provided by the passive BCI.

The future car, thus, presents a highly promising but also challenging environment for BCI applications.

In this paper we present real-world, moving-car EEG recordings of drivers confronted with different types of behaviors from the car's adaptive cruise control (ACC) system. We investigate the detectability of elicited neuroelectric responses amidst unrelated myoelectric and electromagnetic noise. To that end, we use state-of-the-art data cleaning and filtering systems that can also be used online. We present event-related potential (ERP) analyses as well as classification accuracies.

MATERIALS AND METHODS

Participants 15 participants (6 female) aged 24-60 participated. All possessed a valid driver's license for at least three years. They received a monetary reward for their participation. This study was conducted in accordance with the Army Research Laboratory's IRB requirements (DoDI 3216.02).

Experimental Set-Up The experiment was conducted in a modified Toyota Prius, in which a TNO-designed ACC system was installed [15]. The car was driven on the test circuit of the Dienst Wegverkeer Test Centre Lelystad, Netherlands. Other vehicles were present on a larger track surrounding the track but did not interfere with the experimental procedure. The experimenter was present in the backseat of the car during the whole experiment.

We used a 64-channel BioSemi Active-Two to record EEG. We additionally recorded EOG above and below the left eye, ECG, and EMG on the left and right trapezius muscles. Peripheral data is not discussed in this paper (ECG and EOG findings are described [16]). All physiological signals were recorded at a sampling rate of 512 Hz using the same amplifier.

Task and Procedure Participants were told that we are working on automated detection of the driver's desired deceleration settings for an ACC, without requiring the driver to explicitly communicate this desire. We told them that since this is not yet possible, we use a recording of a human voice to represent the desired setting for each trial (i.e. "soft brake please", or "hard brake please"). Participants started with 10 practice trials to get familiar with the task and car dynamics, followed by 300 experimental trials.

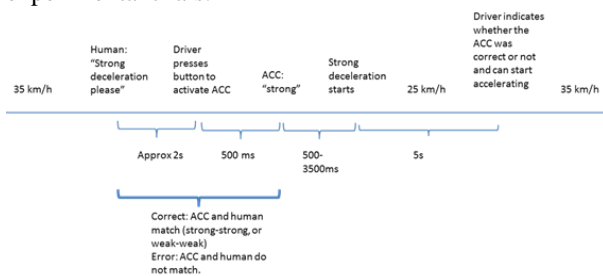


Figure 1: Overview of one trial.

The events constituting one experimental trial are depicted in Figure 1. The car drove at 35 km/h on the track when a human voice indicated the desired deceleration (either soft or hard, in Dutch; 50% chance). The participant pressed down a lever to activate the ACC deceleration. Before executing the deceleration, the ACC announced through a computer voice whether it would decelerate softly or strongly. In 80% of trials, the wish expressed by the human voice was followed (match trial), while in 20% it was not (mismatch trial). A variable time between 0.5 and 3.5 s after the ACC's announcement, the car decelerated to 25 km/h, following either a steep or a shallow velocity profile (i.e. strong or soft deceleration, a maximum deceleration of 3 or 0.7 m/s², respectively; total deceleration time of 0.9 or 2.8 s). Following this, the human voice asked the driver to accelerate again. The driver indicated whether the ACC had followed the desired type of deceleration or not, and pushed the lever up to have the ACC accelerate back to 35 km/h.

Data Processing We used EEGLAB [17] for processing. We compare the data after two different processing paths: "standard" and more rigorously ICA-cleaned data.

Standard preprocessed data was first high-pass filtered at 1 Hz using a Hamming windowed sinc finite impulse response filter. Heavily artifact-contaminated channels were then rejected using the `pop_rejchan` function, based first on kurtosis, and then on probability.

ICA-cleaned data received additional, more rigorous processing. First, the data was high-pass filtered as above at 2 Hz. Artifact subspace reconstruction (ASR; [18]) was used to clean the data. ASR uses a section of clean reference data to compute baseline statistics, and then detects subspaces in continuous data that significantly differ from this reference. It reconstructs the contents of the identified sections using a mixing matrix calculated on the reference data. We used those settings that led to the most rigorous cleaning within the recommended range (burst criterion: 3, window criterion: .05).

Infomax independent component analysis (ICA) on CUDA architecture [19] was applied to the ASR-cleaned data. ICA transforms the mixed-source EEG as recorded in sensor space into time series that are statistically maximally independent (independent components; ICs). Under the assumption that signals from different cortical processes and sources as well as artefactual sources are statistically independent from each other, this method thus transforms the data into 'source space'. ICA results in a transformation matrix, i.e. a filter matrix weighting the individual channels in sensor space, to isolate the different source activities. These independent activities can then be identified and subtracted individually.

The resulting transformation matrix was then copied back to the standard preprocessed data. The additional filtering and ASR cleaning was thus only applied in order to obtain a "clean" transformation matrix. Using this matrix, we then removed artefactual ICs from the standard preprocessed data. In the end, we compare standard preprocessed data versus that same data with artefacts removed through ICA.

Artefactual ICs were identified by manual inspection of their scalp projection and frequency spectrum, as per [20]. Artefactual ICs were removed from the data such that only activity remained that could reasonably be assumed to be cortical. In brief, components were not removed only if they clearly fit two main criteria: a) dipolar, not too superficial projection pattern, and b) clear, smooth peaks in the power spectrum at frequencies known to have clear cortical correlates, mostly below 30 Hz, with no high power beyond those frequencies.

The windowed means approach using regularized shrinkage linear discriminant analysis [21], implemented in BCILAB [17], was used for classification. Data was band-pass filtered between 1 and 15 Hz and segmented into six non-overlapping consecutive time windows of 50 ms each, from 0.2 to 0.5 s after the respective event—a time window that, a priori, could be expected to contain relevant responses to the experimental manipulations. We compare the response to the ACC announcing the upcoming braking behavior (match versus mismatch, strong versus soft), as well as to the actual braking. We used a five-fold nested cross-validation to compute classification accuracy estimates.

ERP analyses include statistics computed per sample between subjects on the amplitude differences of the two classes, using permutation tests with 1000 permutations.

ASR and ICA cleaning was applied to the whole dataset. Cross-validated BCI performance estimates are calculated based on these cleaned sets as an additional measure of potential differences between the sets.

RESULTS

An average of 4 channels (ranging from 0 to 8) were removed from the initial data. From the on average 60 remaining independent components, an average of 8 (ranging from 2 to 14) ICs were identified as being cortical. All others were removed. See figure 2 for a small but representative selection of ICs that were kept.

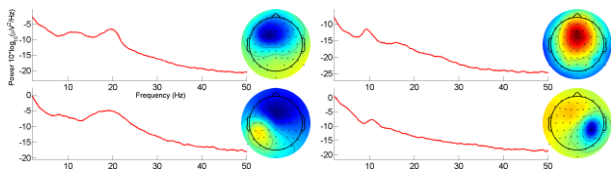


Figure 2: Four ICs that fit the main criteria: spectral peaks in sub-gamma bands and dipolar patterns.

The artefactual noise was not spread evenly across the channels, but was most prominent on parietal and occipital sites. Figure 3 shows grand-average ERPs for the four comparisons. We focus mostly on Oz, a highly contaminated site showing the effect of the ICA cleaning most clearly. To illustrate the vast differences of the noise distribution between the different sites, and the effect on cleaner sites, for one condition, we also present the ERP at the less contaminated electrode Cz. ERPs extracted from standard-preprocessed data are shown on the left; the ICA-cleaned data on the right. Significant differences ($p < 0.05$) are highlighted in grey.

Significant differences can be seen between the peak amplitude around 200 ms in the ICA-cleaned data at electrode Oz comparing the announcement onset of hard versus soft upcoming braking behavior. Also at Oz in ICA-cleaned data, significant differences can be seen around 500 to 600 ms after hard versus soft brake onset. These late differences are most likely due to the experience of the braking itself and not relevant to the driver's mental preparation thereof—thus, we did not update our classification approach to go beyond 500 ms.

Tables 1 to 4 list the individual and mean classification accuracy estimates for the same classifier calibrated on standard-preprocessed data and on ICA-cleaned data for all four comparisons. These results are summarized and discussed in the next section.

CONCLUSION AND DISCUSSION

We have recorded data from 15 participants controlling a moving car. They were confronted with different and sometimes unexpected behavior of the automated driving system, in the form of either strong or soft deceleration. We applied state-of-the-art cleaning and filtering methods in order to investigate the detectability of cortical events amidst the many artifacts produced by the

car itself and the participants' movements.

The ICA cleaning of the data was rigid, removing, in one case, all but only two independent components, and in all cases no less than three-fourths of all components. We see, however, that even in this heavily contaminated data it was still possible to identify cortical activity: we see clear event-related potentials reflecting cortical responses to various driving-related events, on electrodes where the original preprocessed signal was completely drowned out by large-amplitude artifacts (e.g. Oz).

Indeed, even given very large-amplitude artifacts (up to 23 μV on Oz), the relatively small cortical signals ($< 1 \mu\text{V}$ on that same electrode) could be identified with sufficient sensitivity to allow significant differences to become apparent between the classes.

At less contaminated sites, e.g. electrode Cz, we see that the signal is hardly affected even by such rigorous cleaning. The cortical signals remain intact.

The ERP plots show no significant difference between match and mismatch trials. The experimental set-up likely did not make this distinction sufficiently meaningful to the participant to evoke a clearly discriminable signal. Participants were not instructed to pay attention to this, and were occupied by the primary task of driving, so indeed little effect was expected [22].

Because of this, we also see no general classifiability of match versus mismatch events, nor an improvement in classification accuracy after to ICA cleaning. Given the imbalanced number of classes, chance level is at 68% (± 5.2 , $\alpha = 0.05$). Neither standard preprocessed nor ICA-cleaned data is classifiable. We do, however, see an increase in the balance of the classes after ICA cleaning (i.e. the true positive divided by the true negative rate).

Comparing hard versus soft trials, chance level here is 49% (± 5.6 , $\alpha = 0.05$). Time-locked to brake onset, we see a very high classification accuracy of 94% in standard preprocessed data. This decreases significantly after ICA cleaning ($p < 0.01$). This is likely because in the non-cleaned data, strong mechanical and muscular artifacts correlate to these two classes: a steeper braking profile will lead to increased muscular activity and movement. These artifacts are used by the classifier. In the cleaned data, these artifacts are removed and the classifier is only given the activity that was identified to be cortical. This still leads to a classification accuracy of 77%, significantly better than chance.

Time-locked to the onset of the announcement, classification accuracy is 63% without cleaning, and cleaning does not significantly change this ($p = 0.32$). This shows a cortical response to the announcement that is detectable at a single-trial level. The lack of impact on classification accuracy shows that ICA cleaning does not negatively affect these cortical aspects of the data.

The ASR cleaning method can be applied online. Although the precise ICA implementation used here was not online, methods have been developed to calculate ICA transformation matrices online [23]. The two measures on which component selection was based, scalp projection and power spectrum, are thus also available online. It is likely, in fact, that online ICA will give better

results as it can be configured to put more weight on current time windows, making it adaptive to the current context. In [23], the selection of which components to keep and which to remove can be done online but must be done manually. However, (semi)automatic component identification is underway [24].

These methods, thus, allow for strong, rigorous cleaning and filtering of data during continuous, online BCI operation. As we have shown here, these state-of-the-art methods are capable of identifying cortical processes even amidst large-amplitude artefacts that would otherwise drown out the signal of interest.

ICA-based cleaning can target artefactual activity specifically, affecting cortical processes only to a minimal degree. This can provide a large advantage for real-world neuroadaptive technology in realistic settings.

ACKNOWLEDGEMENTS

This research was funded by the U.S. Army Research Laboratory and was accomplished under Contract Number W911NF-10-D-0002.

REFERENCES

- [1] Zander TO, Lehne M, Ihme K, Jatzev S, Correia J, Kothe CA, ... Nijboer F (2011). A dry EEG-system for scientific research and brain-computer interfaces. *Front. Neurosci.*, 5, 53.
- [2] Chi YM, Wang YT, Maier C, Jung TP, Cauwenberghs G (2012). Dry and noncontact EEG sensors for mobile brain-computer interfaces. *IEEE Trans. Neural. Sys. Rehab. Eng.*, 20(2), 228-235.
- [3] Guger C, Krausz G, Allison BZ, Edlinger G (2012). Comparison of dry and gel based electrodes for P300 brain-computer interfaces. *Front. Neurosci.*, 6, 60.
- [4] Debener, S, Minow F., Emkes R., Gandras K, de Vos M (2012). How about taking a low-cost, small, and wireless EEG for a walk? *Psychophysiology*, 49(11), 1617–1621.
- [5] Gargiulo G, Bifulco P, Calvo RA, Cesarelli M, Jin C, van Schaik A (2008). A mobile EEG system with dry electrodes. *IEEE Biomed Circuits Syst* 273-276.
- [6] Zander TO, Kothe, CA (2011). Towards passive brain-computer interfaces: applying brain-computer interface technology to human-machine systems in general. *J Neural Eng*, 8(2), 025005.
- [7] Zander TO, Kothe CA, Welke S, Rötting M (2008). Enhancing human-machine systems with secondary input from passive brain-computer interfaces. In *Proc Graz BCI '08, Graz, Austria*, 144–149.
- [8] Zander TO, Jatzev S (2012). Context-aware brain-computer interfaces: exploring the information space of user, technical system and environment. *J Neural Eng*, (1), 016003.
- [9] Zander TO, Krol LR, Birbaumer NP, Gramann K (2016). Neuroadaptive technology enables implicit cursor control based on medial prefrontal cortex activity. *PNAS*, 113(52), 14898-14903.
- [10] Zander TO, Brönstrup J, Lorenz R, Krol LR (2014). Towards BCI-based Implicit Control in Human-Computer Interaction. In Fairclough SH, Gilleade K (Eds.), *Advances in Physiological Computing* (pp. 67–90). Berlin, Germany: Springer.
- [11] Zander TO, Andreessen LM, Berg A, Bleuel M, Pawlitzki J, Zawallich L., Krol, LR, Gramann, K (2017). Evaluation of a dry EEG system for application of passive brain-computer interfaces in autonomous driving. *Front Human Neurosci*, 11, 78.
- [12] Haufe S, Kim JW, Kim IH, Sonnleitner A, Schrauf M, Curio G, Blankertz B (2014). Electrophysiology-based detection of emergency braking intention in real-world driving. *J Neural Eng*, 11(5), 056011.
- [13] Lin CT, Wu RC, Liang SF, Chao WH, Chen YJ, Jung TP (2005). EEG-based drowsiness estimation for safety driving using independent component analysis. *IEEE Trans Circuits Syst I*, 52(12), 2726–2738.
- [14] Wang YK, Chen SA, Lin CT. (2014). An EEG-based brain-computer interface for dual task driving detection. *Neurocomputing*, 129, 85–93.
- [15] Ploeg J (2014) Analysis and design of controllers for cooperative and automated driving. PhD Thesis, TU/e, Eindhoven, The Netherlands, 2014.
- [16] Brouwer AM, Snelting A, Jaswa M, Flascher O, Krol, LR, Zander, TO (in press). Physiological effects of Adaptive Cruise Control Behaviour in Real Driving. In *Proc. IUI'17, Limassol, Cyprus*.
- [17] Delorme A, Mullen T, Kothe C, Acar ZA, Bigdely-Shamlo N., Vankov A, Makeig, S. (2011). EEGLAB, SIFT, NFT, BCILAB, and ERICA: New Tools for Advanced EEG Processing. *Comput Intell Neurosci*, 2011, 10:10–10:10.
- [18] Mullen T, Kothe C, Chi YM, Ojeda A, Kerth T, Makeig S., ... Jung TP (2013). Real-time modeling and 3D visualization of source dynamics and connectivity using wearable EEG. In *Proc. IEEE EMBC '13, Osaka, Japan*.
- [19] Raimondo F, Kamienskowski JE, Sigman M, Slezak, DF (2012). CUDAICA: GPU optimization of infomax-ICA EEG analysis. *Comput Intell Neurosci.*, 2012, 2:2–2:2.
- [20] Jung TP, Makeig S, Humphries C, Lee TW, McKeown MJ, Iragui V, Sejnowski TJ (2000). Removing electroencephalographic artifacts by blind source separation. *Psychophys* 37(2), 163-178.
- [21] Blankertz B, Lemm S, Treder MS, Haufe S, Müller KR (2011). Single-trial analysis and classification of ERP components. *NeuroImage*, 56(2), 814–825.
- [22] Thurlings ME, van Erp JBF, Brouwer AM, Werkhoven PJ (2013). Controlling a tactile ERP-BCI in a dual-task. *IEEE Trans Comput. Intell. AI Games*, 5(2).
- [23] Hsu SH, Mullen T, Jung TP, Cauwenberghs G. (2014). Online recursive independent component analysis for real-time source separation of high-density EEG. In *Proc IEEE EMBC'14, Chicago, US*.
- [24] Chaumon M, Bishop DV, Busch NA. (2015). A practical guide to the selection of independent components of the electroencephalogram for artifact correction. *J Neurosci Methods*, 250, 47–63.

P	Announce match vs. mismatch							
	Standard				ICA			
	TP	TN	Rat.	Acc.	TP	TN	Rat.	Acc.
1	32	74	0.42	66	44	61	0.72	58
2	25	77	0.33	66	39	74	0.53	67
3	30	74	0.40	66	37	64	0.58	58
4	37	78	0.47	69	48	59	0.82	57
5	32	78	0.41	69	47	73	0.64	67
6	40	76	0.53	69	35	60	0.58	55
7	23	71	0.33	62	33	64	0.52	58
8	25	68	0.37	59	42	59	0.70	56
9	33	70	0.48	62	38	63	0.61	58
10	38	75	0.51	68	43	66	0.65	62
11	30	68	0.44	60	42	56	0.75	53
12	52	85	0.61	78	45	75	0.60	69
13	40	76	0.53	69	43	65	0.66	61
14	30	68	0.44	61	38	59	0.65	55
15	48	79	0.61	72	47	61	0.77	58
	34	74	0.46	66	41	64	0.65	59

Table 1: Classification accuracy estimates for all fifteen participants based on standard-preprocessed data and ICA-cleaned data. Classification distinguished between match versus mismatch trials, time-locked to announcement onset. P = participant number, TP = true positive rate, TN = true negative rate, Rat. = TP/TN, Acc. = combined classification accuracy. Due to class imbalances, chance level is at 68% (± 5.2 , $\alpha = 0.05$).

P	Announce hard vs. soft							
	Standard				ICA			
	TP	TN	Rat.	Acc.	TP	TN	Rat.	Acc.
1	64	61	1.05	63	63	57	1.10	60
2	66	55	1.19	60	66	59	1.13	62
3	47	63	0.75	55	56	59	0.94	57
4	61	59	1.03	60	61	66	0.92	63
5	55	61	0.89	58	52	53	0.99	52
6	57	63	0.89	60	61	59	1.03	60
7	78	74	1.05	76	68	68	1.00	68
8	54	63	0.85	58	62	56	1.10	59
9	49	48	1.01	48	45	55	0.82	50
10	78	69	1.13	74	67	71	0.95	69
11	68	68	1.01	68	58	55	1.06	57
12	72	65	1.10	69	74	67	1.10	71
13	64	73	0.88	68	55	61	0.90	58
14	55	55	0.99	55	62	59	1.06	60
15	59	70	0.85	65	52	55	0.94	54
	62	63	0.98	63	60	60	1.00	60

Table 2: As table 1, with classification distinguishing between hard versus soft brake trials, time-locked to announcement onset. Chance level is at 49% (± 5.6 , $\alpha = 0.05$).

P	Brake match vs. mismatch							
	Standard				ICA			
	TP	TN	Rat.	Acc.	TP	TN	Rat.	Acc.
1	16	69	0.23	59	44	65	0.67	61
2	35	72	0.48	65	37	67	0.54	61
3	31	66	0.47	59	36	61	0.60	56
4	39	73	0.54	66	36	57	0.63	53
5	22	67	0.32	58	28	62	0.46	55
6	27	75	0.36	65	37	64	0.57	59
7	22	69	0.32	59	40	59	0.68	55
8	29	74	0.39	65	33	65	0.51	59
9	31	61	0.51	55	36	63	0.57	58
10	17	73	0.23	61	43	70	0.62	64
11	44	73	0.61	67	44	61	0.72	58
12	28	77	0.37	67	50	67	0.75	63
13	33	64	0.52	58	40	61	0.66	56
14	30	64	0.47	57	47	54	0.86	53
15	38	65	0.57	59	31	59	0.53	54
	29	69	0.43	61	39	62	0.62	58

Table 3: As table 1, with classification distinguishing between match versus mismatch trials, time-locked to brake onset.

P	Brake hard vs. soft							
	Standard				ICA			
	TP	TN	Rat.	Acc.	TP	TN	Rat.	Acc.
1	94	85	1.10	89	91	79	1.16	85
2	99	90	1.10	95	79	74	1.07	77
3	87	85	1.02	86	68	69	0.99	69
4	98	93	1.05	96	80	72	1.11	76
5	95	94	1.01	95	65	68	0.96	67
6	99	90	1.10	94	75	77	0.97	76
7	99	96	1.03	98	79	69	1.14	74
8	95	83	1.15	89	67	64	1.05	65
9	99	94	1.05	96	96	90	1.07	93
10	97	90	1.08	94	93	85	1.10	89
11	88	79	1.11	83	88	72	1.22	80
12	100	99	1.01	99	82	76	1.07	79
13	100	98	1.02	99	68	62	1.09	65
14	99	99	1.01	99	75	67	1.13	71
15	99	96	1.04	97	92	79	1.17	85
	97	91	1.06	94	80	73	1.09	77

Table 4: As table 2, with classification distinguishing between hard versus soft trials, time-locked to brake onset.

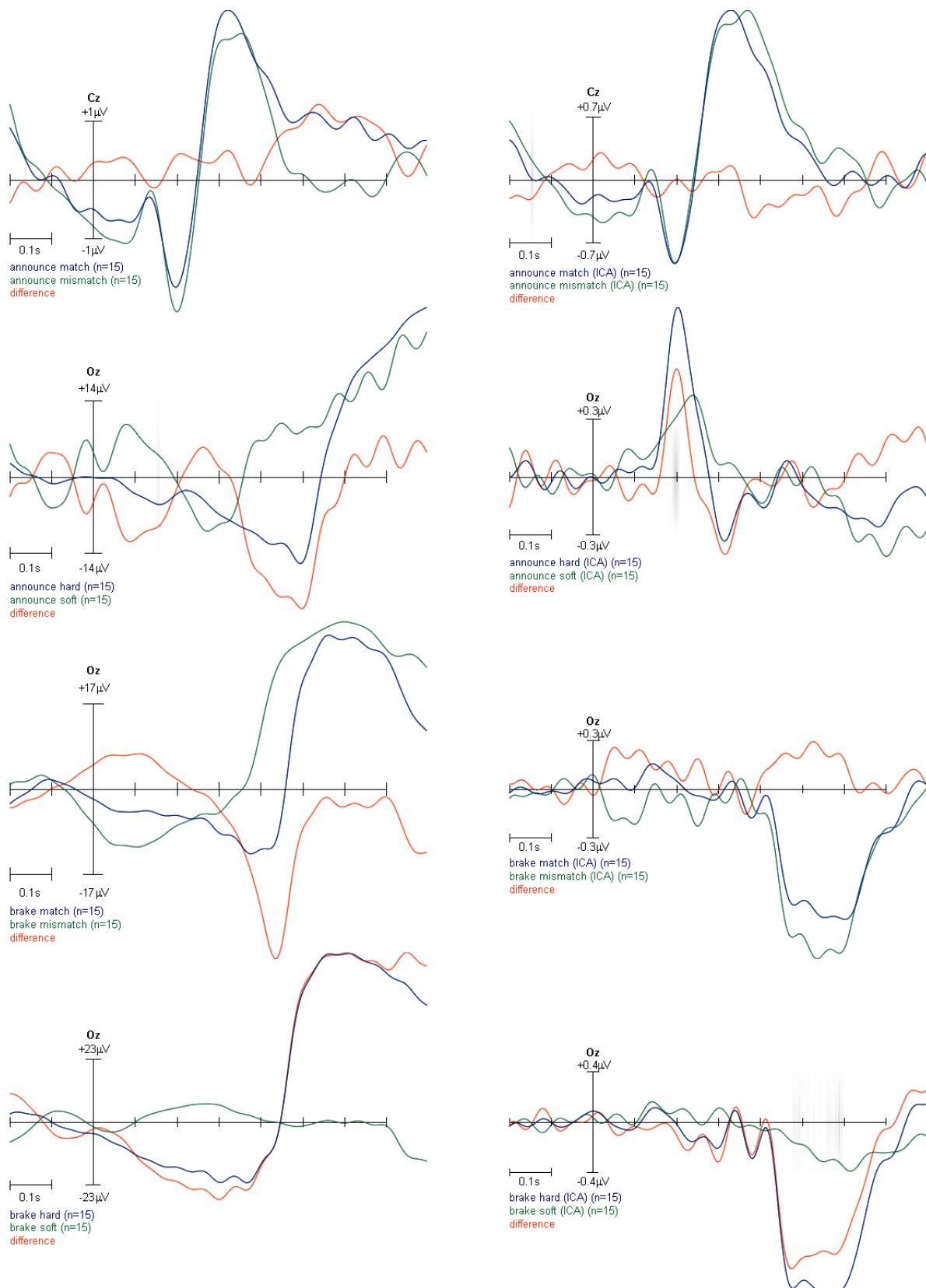


Figure 3: Grand average ($n=15$) event-related potentials of standard-preprocessed (left) and ICA-cleaned data (right). Top to bottom: ERP at Cz time-locked to the ACC announcement onset of the upcoming braking behavior, match versus mismatch trials; ERP at Oz time-locked to the same, announcing “hard” versus “soft”; ERP at Oz time-locked to the onset of the braking behavior itself, match versus mismatch trials; ERP at Oz time-locked to the same, hard versus soft braking. Significantly different samples are highlighted in grey, modulated by p-values (lower p-value = darker grey).

© 2017

Verlag der Technischen Universität Graz

<http://ub.tugraz.at/Verlag>



ISSN 2311-0422

ISBN 978-3-85125-533-1

DOI 10.3217/978-3-85125-533-1